Influence of Xe and Kr impurities on x-ray yield from debris-free plasma x-ray sources with an Ar supersonic gas jet irradiated by femtosecond near-infrared-wavelength laser pulses

V. L. Kantsyrev, K. A. Schultz, V. V. Shlyaptseva, G. M. Petrov, A. S. Safronova, E. E. Petkov, J. J. Moschella, I. Shrestha, W. Cline, P. Wiewior, and O. Chalyy

Phys. Rev. E **94**, 053203 — Published 7 November 2016

DOI: 10.1103/PhysRevE.94.053203

Influence of Xe and Kr impurities on x-ray yield from debris-free plasma x-ray sources with an Ar supersonic gas jet irradiated by femtosecond near-infrared-wavelength laser pulses

V.L. Kantsyrev[1], K.A. Schultz[1], V.V. Shlyaptseva[1], G.M. Petrov[2], A.S. Safronova[1], E.E. Petkov[1], J.J. Moschella[1], I. Shrestha[1], W. Cline[1], P. Wiewior[1], O. Chalyy[1]

[1] *Physics Department, University of Nevada, Reno, Nevada 89557, USA*

[2] *Plasma Physics Division, Naval Research Laboratory, Washington, DC 20375, USA*

Abstract. Many aspects of physical phenomena occurring when an intense laser pulse with sub-ps duration and an intensity of 10^{18}-10^{19} W/cm^2 heats an under-dense plasma in a supersonic cluster/gas jet were studied to determine the relative contribution of thermal and non-thermal processes to soft and hard x-ray emission from debris-free plasmas. Experiments were performed at the University of Nevada Reno (UNR) Leopard laser operated with a 15 J / 350 fs pulse and different pulse contrasts (10^7 or 10^5). The supersonic linear (elongated) nozzle generated Xe cluster/monomer jets as well as jets with Kr/Ar or Xe/Kr/Ar mixtures with densities of 10^{18} - 10^{19} cm^{-3}. Prior to laser heating experiments, all jets were probed with optical interferometry and Rayleigh scattering to measure jet density and cluster distribution parameters. The supersonic linear jet provides the capabilities to study the anisotropy of x-ray yield from laser plasma, and also laser beam self-focusing in plasma which leads to efficient x-ray generation. Plasma diagnostics included x-ray diodes, pinhole cameras, and spectrometers. Jet signatures of x-ray emission from pure Xe gas, as well as from a mixture with Ar and Kr, were found to be very different. The most intense x-ray emission in the 1-9 KeV spectral region was observed from gas mixtures rather than pure Xe. Also, this x-ray emission was strongly anisotropic with respect to the direction of laser beam polarization. Non-local thermodynamic equilibrium (Non-LTE) models have been implemented to analyze the x-ray spectra to determine the plasma temperature and election density. Evidence of electron beam generation in supersonic jets plasma was found. The influence of the sub-ps laser pulse contrast (a ratio between the laser peak intensity and pedestal pulse intensity) on the jets' x-ray emission characteristics is discussed. Surprisingly, it was found that the x-ray yield was not sensitive to the pre-pulse contrast ratio.

I. Introduction

Short pulse lasers can be used for the production of short bursts (nanoseconds) of debris-free x-rays in a wide spectral range (1-20 keV) by irradiating underdense plasmas or clusters. This is not only of pure scientific interest but may also lead to many useful applications involving x-rays such as x-ray effects testing, backlighting, lasers and high-harmonic generators. In this paper the emphasis is on investigating the influence of high-atomic-number gas impurities (Kr and Xe) in Ar carrier gas on x-ray yield. The pure Xe and Kr/Ar and Xe/Kr/Ar mixture jets were irradiated by sub-ps (350 fs) laser pulses with different contrast ranging from 10^5 to 10^7 (measured as a ratio between the laser peak intensity and the pedestal pulse intensity) at laser intensity in the focus spot around

10^{19} W/cm^2. We applied a linear (elongated) nozzle that generated a cluster/monomer supersonic linear jet, which allows us to study the anisotropy of x-rays from the laser plasma, as well as the possibility of laser beam self-focusing research in the plasma, which is critical for efficient x-ray generation as was demonstrated in Ref. [1]. Measurements of the plasma were made, and include x-ray spectra and pinhole images, time-resolved x-ray bursts, and electron beams. Prior to laser heating experiments, characterization of linear supersonic gas jets was performed through measurements of the gas jet density via interferometry and of the cluster distribution parameters via Rayleigh scattering. A non-LTE Collisional Radiative Equilibrium (CRE) model was used to extract the electron temperature and density of laser-produced plasma from experimental spectra.

A debris free cluster/gas medium as a sub-ps laser target has the advantages of both solid and gaseous targets [2]. For example, targets consisting of a layer of nanotubes on the top of flat surfaces produce debris in form of ion and electron beams, and also solid micro-particles and liquid droplets when x-ray bursts are generated [3]. Clusters appear as a result of spontaneous condensation in a super-cooled high-pressure gas jet from a nozzle. The target is considered to be a medium which consists of the continuous gas phase and the discrete condensed phase clusters [2]. Typically, in jets with an average density of 10^{18} - 10^{19} cm^{-3}, the clusters' diameter is several tens of Å with 10^3-10^4 atoms per cluster. At high intensity, the laser converts the cluster into a ball of hot dense plasma whose lifetime τ_c is limited by hydrodynamic expansion or Coulomb explosion. The plasma in the cluster/gas target is created when the atoms are ionized by laser radiation (with pulse duration τ_{las}) via resonant heating of electrons, optical field ionization, and tunnel ionization ($\tau_{las} < \tau_c < 1$ ps) [2]. These processes create highly charged ions that are excited by the background electrons and emit x-rays.

In many experiments it was demonstrated that when pure Ar [4, 5], Kr [6], Xe [7, 8], or a Kr/Ar [9] mixture, irradiated by fs laser pulses with wavelength near 1 μm, the gas/cluster jets become efficient x-ray sources. In this work we show that Xe/Kr/Ar mixture jets generate more powerful x-ray bursts and in a broader spectral range. We also show that in contrast to previous studies with pure gas jets (Ar, Kr, Xe) [2, 10, 11], there is no correlation between lower laser contrast and smaller x-ray yields.

The initial idea about increasing the x-ray generation efficiency of the Xe/Kr/Ar mixture was based on the possibility of improving the cluster ionization efficiency and, consequently, the x-ray yield from laser irradiated gas jets by adding easily ionizable seed atoms (Kr and Xe) to the lighter carrier gas (Ar) because: 1) clusters formed from Kr or Xe (in Xe/Kr/Ar mixture jet) might have

higher starting electron density n_e produced by the initial laser ionization than pure Ar clusters (due to lower ionization potential of outer electron shells of Kr and Xe compared with Ar); 2) the x-ray spectra of gas mixtures cover a broader spectral range compared to pure Ar or Kr jets; and 3) the internal degrees of freedom of the heavier seed gas are cooled by the carrier gas (Ar), promoting more efficient clustering in the seed gas [12, 13].

The paper is organized as follows. Experimental details are described in Section II. Results of the characterization of linear jets with optical diagnostics are in Section III. Theoretical studies of x-ray emission from Xe jets are presented in Section IV. Results of experiments on the study of x-ray emission from linear jets are described in Section V. The discussion and conclusion are given in Section VI.

II. Experimental details.

The experiments were conducted on the UNR 40 TW Leopard laser facility. The Leopard laser is a hybrid Ti-Sapphire/Nd-glass laser system with a 1057 nm wavelength, pulse duration 350 fs and 10-15 J output energy. The laser pulse pedestal was about 15 mJ with duration 3 ns (main pulse was positioned in the pedestal middle). The laser pulse contrast (ratio between the laser peak intensity I_{peak} and the pedestal pulse intensity I_p) in most studies was around 10^7, but in some experiments it was changed to 10^5. The maximum intensity of laser radiation in the 10 μm diameter focusing spot was about 10^{19} W/cm^2.

In the experiments described below, a linear nozzle was implemented (Fig. 1). The linear supersonic nozzle (exit cross-section is 1.5 x 3 mm) was mounted to Series 9 (Parker Co., USA) pulsed gas valve with 350 μs response time and backing pressure P ~ 500-700 psi (30-45 atm.). This linear nozzle produces a Mach 4 gas jet, high density, and temperatures as low as 100 K, i.e. conditions well suited to generate clusters in the gas jet. We were able to vary the gas delay timing and backing pressure on the valve to change the density and shape of the gas jet. The gas delay time was defined as the interval between energizing of the pulsed valve and the moment the laser pulse interacts with the gas jet. In these experiments gas jets with different compositions were studied: pure Xe, a 15%Kr/85%Ar mixture, and two different mixed gas jets: XeKrAr I (13% Xe-19% Kr-68% Ar) and XeKrAr II (8% Xe-12% Kr-80% Ar) [percentage is in partial pressure].

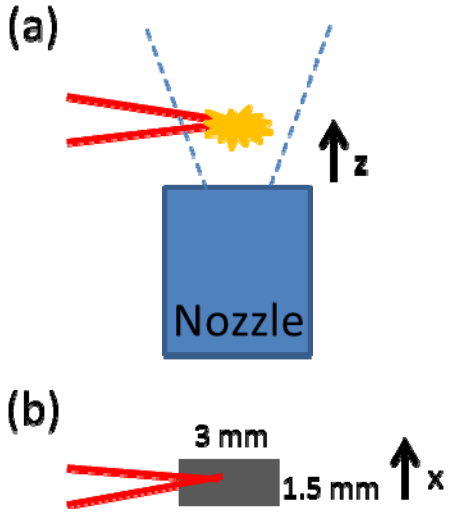

Fig.1. (Color on-line). Schematic of the experiment with linear supersonic nozzle: (a) side view; (b) view along central jet axis. Laser beam (solid lines to the left) focused by a parabolic off-axis laser mirror is shown in red, cluster/gas jet boundaries are marked with dashed line, and laser-produced plasma is in yellow. Laser beam polarization is directed along the Z axis.

The linear supersonic nozzle was placed on a 3D translational mount in the center of the vacuum chamber (operational vacuum $5x10^{-5}$ torr), which is the target area of the Leopard laser. The diagnostics include both time-resolved and time-integrated devices (Fig. 2). Time-resolved x-ray diagnostics consist of three sets of filtered x-ray detectors. Each set included absolutely calibrated diamond photoconducting detectors (PCD) with response time 0.5 ns and filter cut-off energy 2.4 keV, and three cross-calibrated AXUV-HS5 Si-diodes with response of time 1 ns and filter cut-off energies of 1.4, 3.5 and 9 keV. The filter cutoff energy $E_{1/e}$ (defined by the 1/e transmission of the filter where e is the base of natural logarithm) denotes a lower boundary to the radiation incident on the filtered detectors. Two Faraday cup detectors with 4 μm Al filters (electron cut-off energy was 19 keV) were used for electron beam studies. The timing of all these detector signals was measured in correlation with the gas delay time. Time-integrated x-ray diagnostics include two three-channel pinhole cameras (cut-off energies 0.7, 1.4 and 3.5 keV) with spatial resolution 60 μm. We also installed a Johann type x-ray spectrometer (spectral resolution $\lambda / \Delta\lambda = 1200$) with a Si crystal. The two horizontal sets of time-resolved diagnostics were placed perpendicular to the laser beam polarization, one aligned near 15° with respect to laser beam propagation direction and the second set at 90° with respect to laser beam propagation. The vertical group was placed in a direction parallel to the laser beam polarization (Z axis) and the jet propagation. The pinhole cameras and Faraday cups were typically in the 15° horizontal and vertical packages. The X-ray spectrometer was positioned near the horizontal group at 90° to the laser beam polarization and propagation.

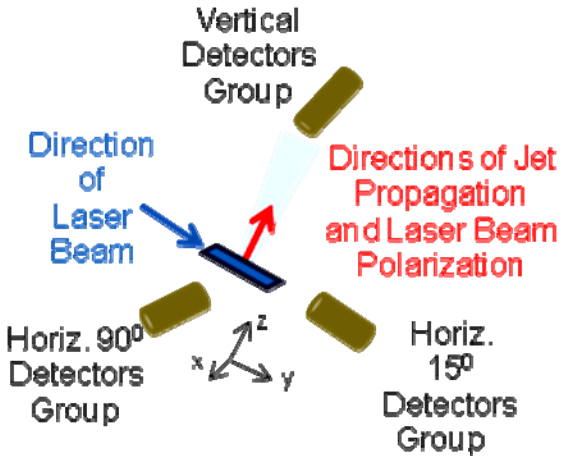

Fig. 2. (Color on-line).Schematic of x-ray and electron beam diagnostic positions in the experiment with the linear nozzle. Vertical detector group is along Z axis, horizontal 90° detector group is along x-axis, horizontal 15° detector group is directly 15° clockwise from Y axis in X-Y plane.

We performed multiple experimets for each time delay of studied gases. Typically, there were three consistent laser shots that confirm the reproducibility of our results.

Note that during preliminary experiments, it was found that maximum x-ray yield corresponds to a 1 mm distance between the focus of laser beam and the exit of the linear nozzle [9].

III. The characterization of linear gas-puff jets before laser heating experiments.

Prior to the laser heating experiments, characterization of the linear gas jets was performed via a combination of optical interferometry and a Rayleigh scattering system as was done in Ref. 14. Interferometry is a common laser based diagnostic that can be used to measure gas densities. The actual interferometric measurement yields the phase shift of the laser light integrated along the path of the laser beam. 2D interferograms were captured using a standard Mach-Zehnder arrangement where a pulsed laser (wavelength - 532 nm, 6 ns pulse duration) was used. Fig. 3 shows examples of line-integrated density profiles for two gas jets: pure Xe and mixture XeKrArI. For both jets the gas density decreases rapidly with distance from the nozzle, which in Fig. 3 is located at Z=0. The optimal combination for getting maximum density at 1 mm from nozzle of pure Xe and Xe/Kr/Ar mixtures was around 550 - 600 psi (~40 atm.) backing pressure with 1 ms delay time. The typical width of the gas jet is around 2.7 mm at a distance of 1 mm from the nozzle (z axis direction) and is relatively independent of gas type and delay time. The maximum average jet densities at 1 mm from the nozzle (position of laser beam focusing point) were calculated based on experimental data by taking the line-integrated density divided by the width of gas jet in the orthogonal direction. For example, for pure Xe it was $N_{Xe} = 2.14 \times 10^{19}$ cm^{-3} and for mixture XeKrArI was $N_{XeKrArI} = 1.94 \times 10^{19}$ cm^{-3}.

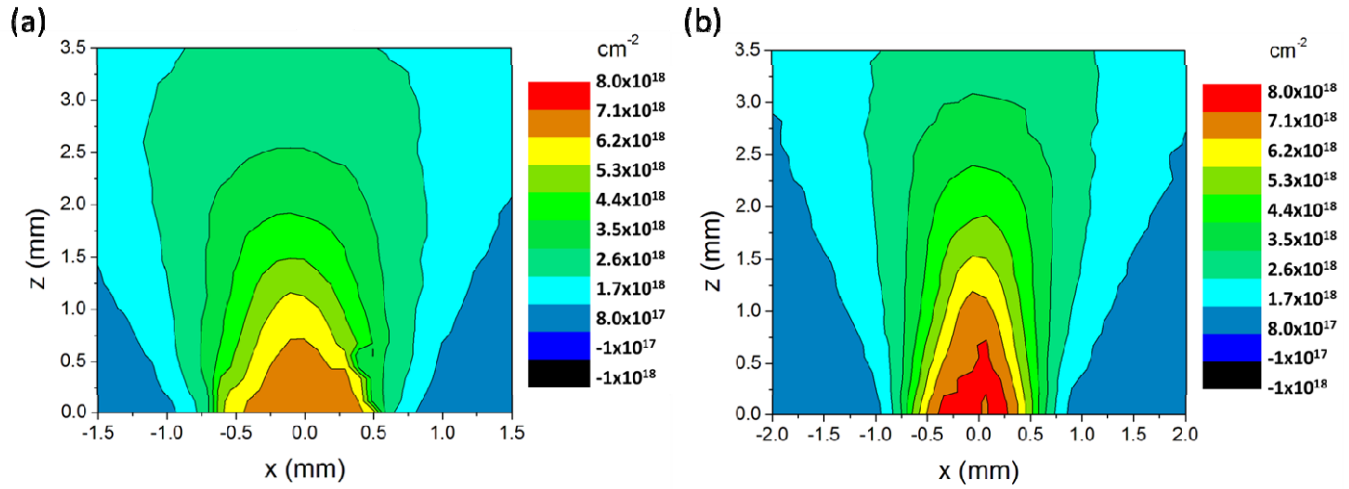

Fig. 3. (Color on-line). Line-integrated density profiles: (a) pure Xe (backing pressure – 550 psi, delay time – 1000 μs); (b) mixture XeKrAr II: 8% Xe, 12% Kr, 80% Ar (backing pressure – 600 psi, delay time – 1000 μs).

The Rayleigh scattering system was applied to determine the main cluster parameter ηN_c that allows us to retrieve the average cluster radius $R_{cluster}$ within the jet according to $R_{cluster} \approx (N_c)^{1/3} R_{atom}$, where R_{atom} is the average radius of an atom in a cluster, η is the fraction of atoms in the cluster state and N_c is the average number of atoms in the cluster. For the scattering setup, we used a continuous 2W diode laser (wavelength - 445 nm) in conjunction with a gated intensified charge coupled device (ICCD) camera. The scattering optical signal was relatively easy to observe using the supersonic nozzle.

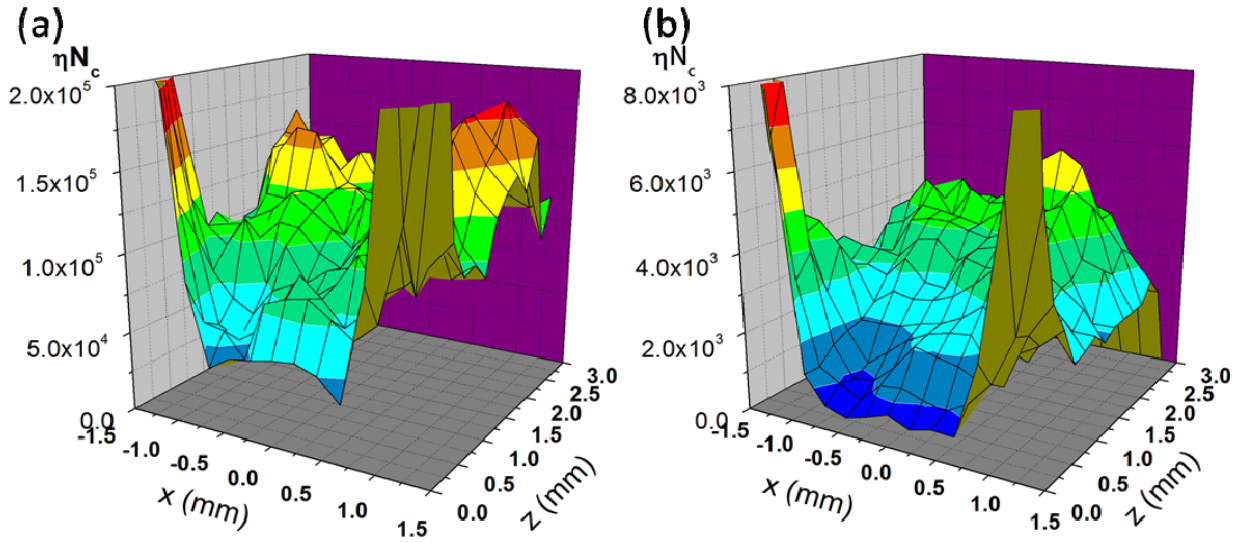

Fig. 4. (Color on-line). Measured profiles of cluster parameter ηN_C for: (a) pure Xe, and (b) XeKrArI [13% Xe-19% Kr-68%] mixture linear jets with backing pressure 550-600 psi and the same time delay (830 μs). Axis X and Z are as in Fig. 1. View of the Rayleigh scattering system is along nozzle exit cross-section longitudinal axis. In the calculations of ηN_c, the magnitude of the signal of reflected light is divided by the density of the gas jet in each area. There is a high

gradient in density at the edges of the gas jet and, as such, a very low density of gas surrounding the main jet. We attribute the large increase in ηN_c to the low density numbers outside the jet in the denominator of the calculations.

The cluster parameter was measured at the optimum distance from the linear nozzle exit (1 mm). In pure Xe it was much larger than that of the Xe/Kr/Ar mixtures (Fig. 4) and that of the other gases. The calculated cluster radii for the pure gases are as follows: $R_{cluster}(Xe)=49Å$, $R_{cluster}(Ar)=16Å$, $R_{cluster}(Kr)=14Å$. Radii of the pure gas clusters were determined by assuming that all atoms are clustered ($\eta=1$). In the case of mixed gases, η is less than one. Spectroscopic analysis has shown previously (Ref. 10) that the Ar atoms in the gas jet do not cluster. Further studies will need to be performed in order to determine what percentage of the mixed gases are clustered; however, we do conjecture that each gas (Kr or Xe) in the mixtures cluster independently due to their non-reactivity as noble gases. Alternatively, the line-integrated density of Xe/Kr/Ar mixtures was higher compared with pure Xe at the same distance (Fig. 3).

As is well known, x-ray radiation produced using short pulse lasers is often accompanied by high-energy debris projectiles, which can be detrimental to surrounding equipment and test subjects. Our experiments conclusively showed that laser irradiated cluster/monomer jets are debris-free sources of x-ray radiation. This was verified by inserting thin metal objects (several μm thick Al, Ti, or Cu foils) near the laser focusing point in jets (1-2 cm distance) oriented at 90° to laser beam axis. On all tested foils, we found only thermal and ion beam damages from the plasma, but no holes from solid fragments and liquid droplets that are typically generated by solid targets [3, 15]. These results were a testimony for the lack of debris, which was a significant improvement compared to analogous experiments with thin flat laser targets where many holes appeared after the first laser shot [15].

IV. Theoretical modeling of interaction of sub-ps laser pulses with Xe linear jets.

A 3D relativistic Molecular Dynamics (MD) code [16, 17] was used for modeling the interaction of fs laser pulses with Xe clusters. The plasma formation within the cluster, coupling of laser energy to the plasma, and plasma evolution are all intricate parts of the model. The MD model accounts for ionization of the atoms/ions inside the cluster due to optical field and collisional ionization with electrons to calculate the ion charge distribution f(q). The cluster radius $R_{cluster}(t)$ is calculated from the particle positions. From f(q) and $R_{cluster}(t)$ the ion densities $n_i(q,t)$ of any charge state q can be computed at any given time.

Numerical simulations were performed for Xe clusters. Their initial density is that of liquid Xe. The initial cluster radius was 5 nm (50 Å, see chapter III) corresponding to 6144 atoms per cluster, and the initial charge was set to zero (neutral atoms). Periodic boundary conditions were used to account for the presence of adjacent clusters. The inter-cluster distance was 50 nm, about ten times the initial cluster radius.

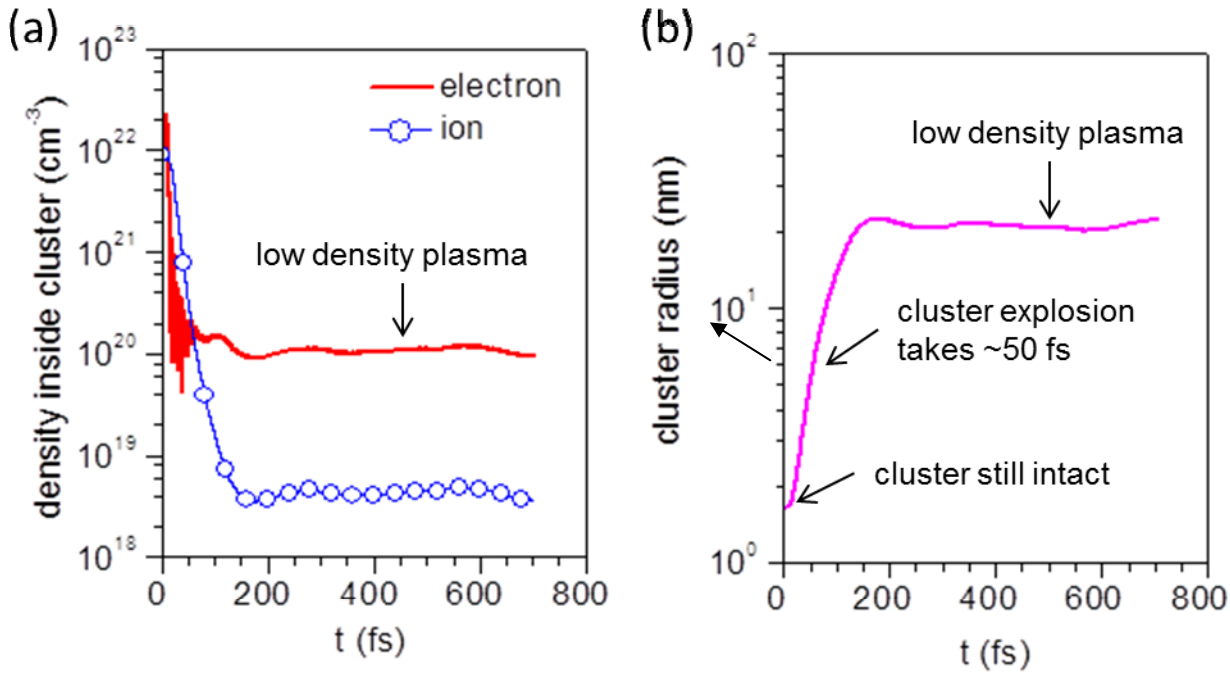

Fig. 5. (Color on-line). Simulation results of sub-ps laser pulse interacting with Xe clusters. Time evolution of the (a) electron and ion densities inside the cluster and (b) cluster radius. Laser parameters: peak intensity 10^{19} W/cm^2, pulse duration 350 fs (FWHM), wavelength 1 μm. Xe cluster initial density is 1.2×10^{22} cm^{-3}.

The numerical simulations show that the interaction of laser radiation with clusters lasts about 100 fs (Figs. 5 and 6). After only 30-50 fs the cluster starts to expand. The cluster expansion accelerates and the electron and ion densities (and cluster density) decrease by 3-4 orders of magnitude and levels off at density equal to the gas density. The decomposed clusters form uniform plasma. For t >100-120 fs the x-ray generation is the result of laser pulse interaction with a hot low density Xe plasma as in a gas jet without clusters. There is, however, a profound difference between them. Sequential ionization (optical field and collisional) gradually increases the ion charge and produces highly charged ions, from which soft and harder x-ray emission (> 200-300 eV) is observed. However, as seen in Figs. 5 and 6, ions with charge $q > 9$ -12 are created only after time $t >$ 15-30 fs,

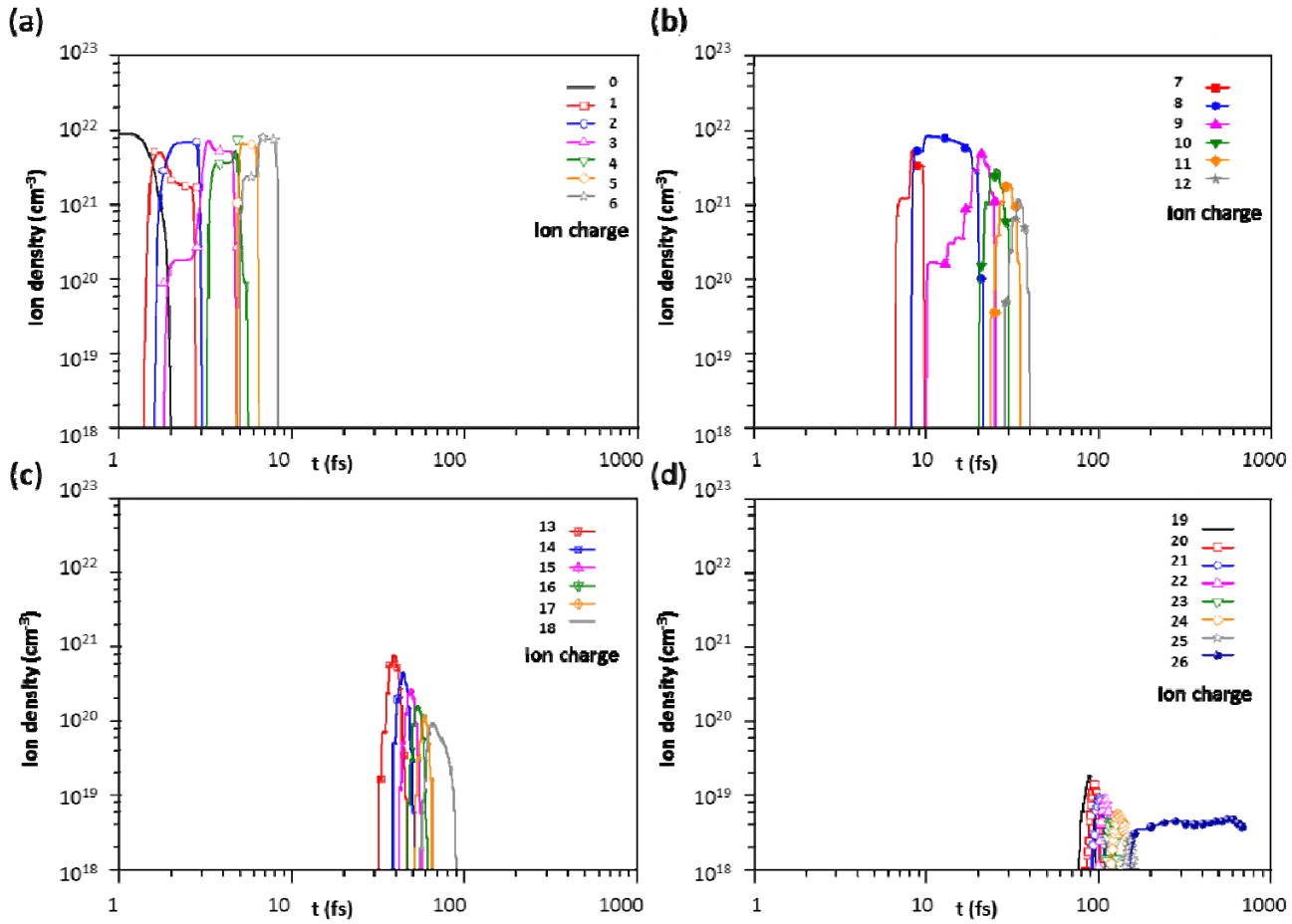

Fig. 6. (Color on line). Time evolution of Xe ion densities with ion charge *q* from: (a) 0 to 6, (b) 7 to, (c) 13 to 18, and (d) 19 to 26.

when cluster expansion has taken place and the ion density starts to decrease. As a result, later in time, ions with a charge of up to Xe^{26+} are produced with decreasing density, which asymptotically approaches the density of the gas. The only ion left standing after t>150 fs is with charge q=26 because ionization stalls at closed shell: the next ionization potential is very large, I_p=1.4 KeV, and all ions pile up at charge q=26. Clusters can absorb a large fraction of the laser radiation even though clusters exist only for a very brief period of time.

V. X-ray emission study from linear jets irradiated by sub-ps laser pulse.

Experiments were performed mainly with two different mixed gas jets denoted for brevity as XeKrArI: 13% Xe-19% Kr-68% Ar, and XeKrArII: 8% Xe-12% Kr-80% Ar (% is in pressure), as well as a pure Xe jet. In some measurements 15%Kr/85%Ar jets were used for comparison. The x-ray bursts from pure Xe and Xe/Kr/Ar mixture jets lasted from 2 to 7 ns, which is longer than x-ray

detectors' response time: 0.5 ns for the PCD and 1 ns for Si x-ray diodes. In all spectral regions, the shape of the x-ray bursts was similar: a sharp forefront, and a gently sloping trailing edge (Figs. 7 and 8). The sharp forefront appears as a result of the "instantaneous" (<1 ps) energy absorption during the laser pulse, which is much shorter than the x-ray detection time (1 ns). The gently sloping trailing edge is most likely due to a radiative cooling of the (expanded) plasma, which continues on a nanosecond time scale. We were unable to estimate the actual duration of x-ray burst forefront due to low time resolution of our x-ray detectors (0.5-1 ns).

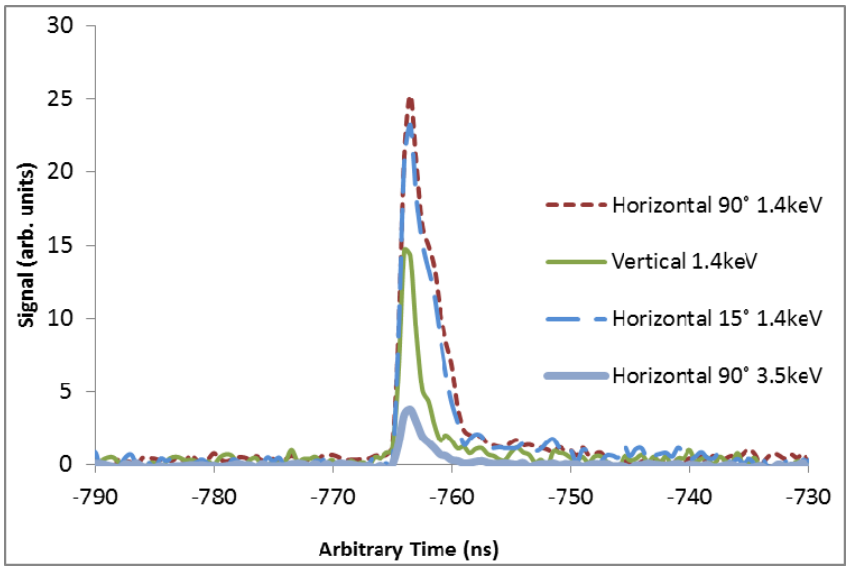

Fig. 7. (Color on-line). Unnormalized x-ray bursts from pure Xe jet at 10^{19} W/cm^2. Shot #1595.

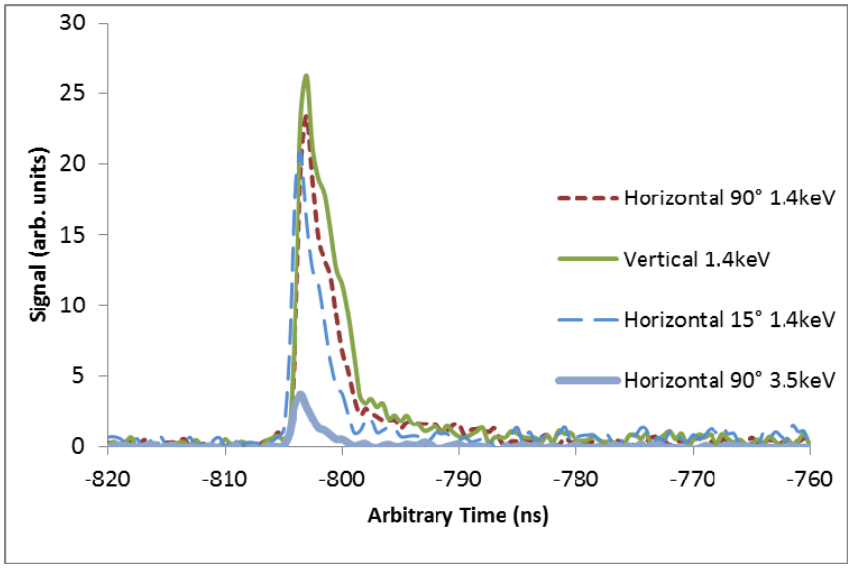

Fig. 8. (Color on-line). Unnormalized x-ray bursts from pure XeKrAr I mixture jet at 10^{19} W/cm^2. Shot #1584.

Laser heating experiments at 10^{19} W/cm^2 have shown that XeKrArI and XeKrArII mixture jets produced similar x-ray spectra, as shown in Fig. 9.

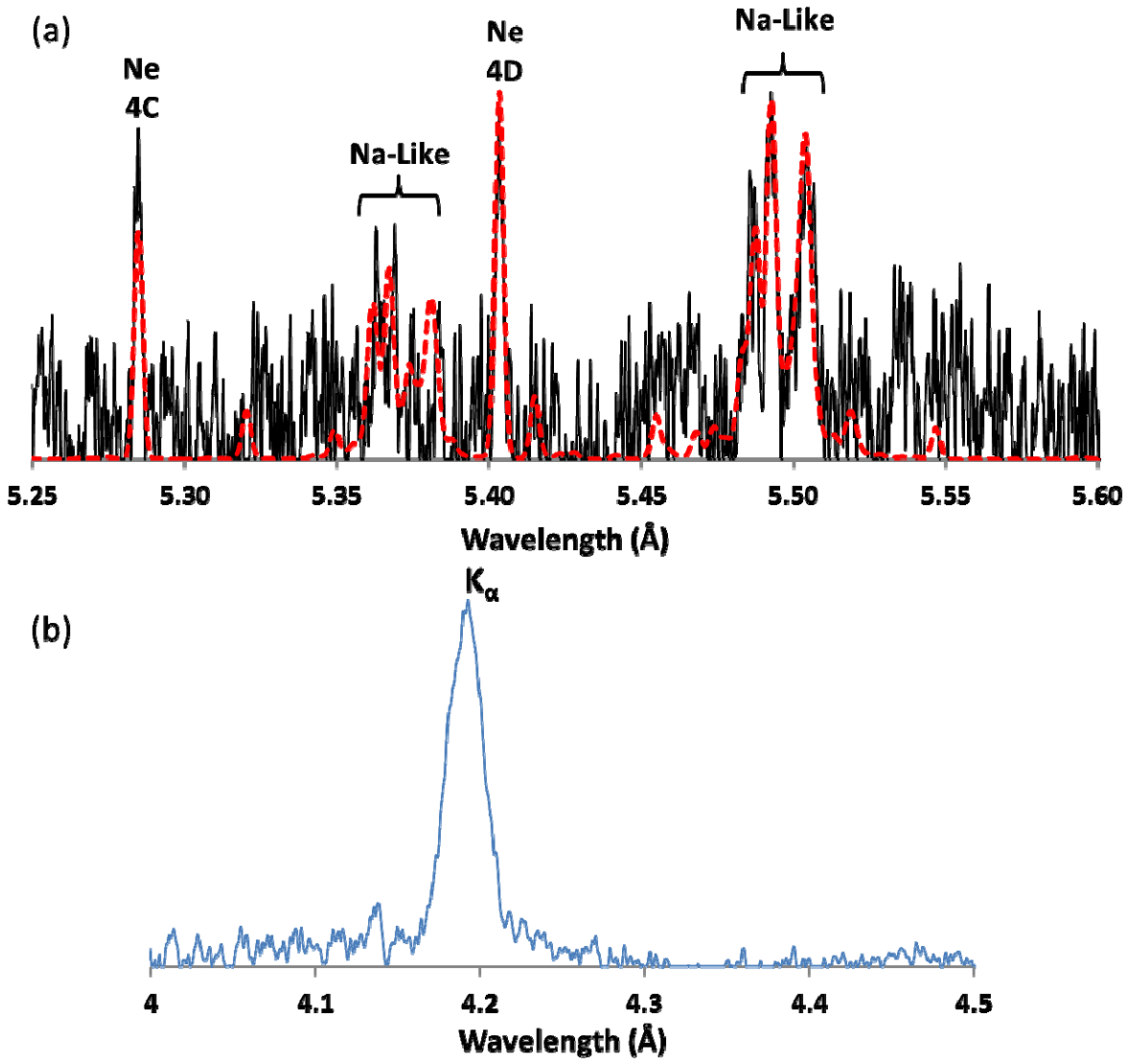

Fig. 9. (Color on-line). (a) L-shell Kr x-ray spectra fit with modeling (dashed line) and (b) "cold" Kα Ar x-ray line obtained with Johann spectrometer from XeKrAr I jet irradiated at intensity 10^{19} W/cm^2 (shots # 1586 and # 1585 respectively, delay time 830 μs, backing pressure 600 psi).

The non-LTE Collisional Radiative (CR) model for Kr [9] was used for identification of Kr lines and estimation of plasma parameters. For L-shell Kr plasmas from gas mixture XeKrArI, we calculated an electron temperature and density T_e =450 eV and n_e=10^{21} cm^{-3}, respectively (same as was observed in [9] for 15%Kr/85%Ar jet plasma). Similar results were obtained for XeKrArII jet plasma. From these Xe/Kr/Ar mixtures, argon radiated only the "cold" Kα lines (same as in [10] for

15%Kr/85%Ar jet plasma) which confirms that in supersonic jets of such mixtures, Ar carrier gas generates clusters inefficiently or has not clustered at all, as was predicted in Ref. [12]. For Xe, we only obtained strong unresolved x-ray spectra in the 2.7-3.0 Å (4.6-4.1 keV) spectral region. To improve detection, a more sophisticated x-ray spectrometer will be deployed in the future.

The x-ray spectra of the gas mixtures cover a broader spectral range compared to pure gas jets. For example, our observations in 2-5 keV region at 10^{19} W/cm^2 have already shown that the Xe/Kr/Ar source (with Xe concentration lower than 15 %) covers at least the 2.2 – 4.6 keV field, and Kr/Ar source covers the 2.2-3 keV field [9]. For comparison, pure Ar source radiates strong line spectra near 3.1 – 3.2 keV [9], and pure Kr source covers a range of 2.2-2.4 keV [9].

For the preliminary estimation of maximum possible value of coefficient of conversion for laser energy to x-ray (ε) in wide sub-keV spectral region, XeKrArI jet laser heating experiments with a horizontal PCD detector (at 15^0) filtered by 1 μm thick aluminized mylar filter (0.7 keV cutoff energy) were performed. This coefficient of conversion was found to be $\varepsilon \sim 10^{-3}$.

A systematic comparison of x-ray yields from pure Xe, Xe/Kr/Ar, and Kr/Ar jets in a spectral region > 2.4 keV (suitable for many practical applications, such as x-ray backlighting) is shown in Table 1. The experimental error of the measurements was estimated to be ± 15 %. The observed emission from mixture XeKrArI was 19% higher than XeKrArII, 21% more than Kr/Ar, and 38% stronger than pure Xe.

Gas jet type	Horizontal PCD at 15^0 mJ / ε	Vertical PCD mJ / ε
15%Kr/85%Ar	4.2 / 2.8 x 10^{-4}	1.6 / 1.1 x 10^{-4}
Xe	3.7 / 2.5 x 10^{-4}	1.2 / 8 x 10^{-5}
13%Xe/19%Kr/68%Ar	5.1 / 3.4 x 10^{-4}	2. 3 / 1.5 x 10^{-4}
8%Xe/12%/Kr/80%Ar	4.3 / 2.9 x 10^{-4}	1.6 / 1.1 x 10^{-4}

Table. 1. Average total energy in mJ emitted in 4π solid angle and average ε (coefficient of conversion laser energy to x-ray) in spectral region > 2.4 keV measured with absolutely calibrated PCD detectors (delay time 830 μs, backing pressure 600 psi) at 10^{19} W/cm^2.

Data from Table 1 demonstrated an interesting and somewhat unexpected phenomenon: the x-ray radiation in spectral range > 2.4 keV from XeKrArI, XeKrArII, Xe and 15%Kr/85%Ar jets is emitted anisotropically with maximum radiated perpendicular to the laser beam polarization. The degree of anisotropy (ratio of "horizontal" to "vertical" yields) is about 2.5 - 3. Since in the region of x-rays harder than 2.4 keV the mixture XeKrArI radiated better than XeKrArII, and since both mixtures produced similar x-ray spectra (see for example Fig. 9), the study continued with the XeKrArI mixture jet.

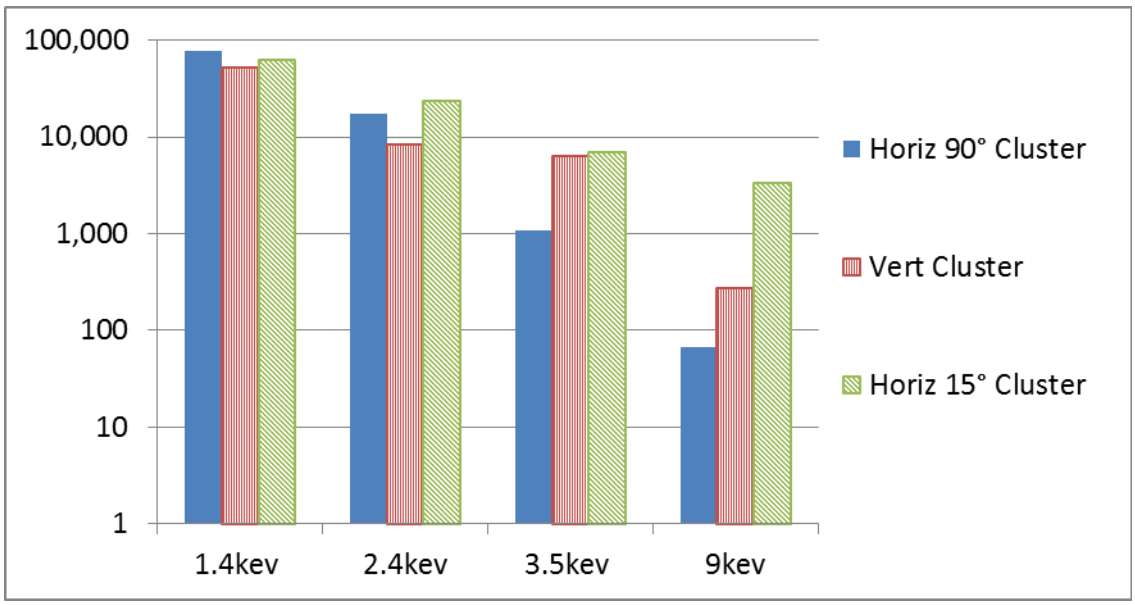

Fig. 10. (Color on-line). Normalized spectral integrated distribution of x-ray emission (that includes line, recombination, and bremsstrahlung radiation) from XeKrAr I jet (shot #1584) in wide spectral range at laser beam intensity 10^{19} W/cm^2. Vertical axis shows x-ray intensity in arbitrary units, horizontal axis shows x-ray photons energy in keV. Term "cluster" in this illustration means group of x-ray detectors. Delay time 830 μs, backing pressure 600 psi.

The investigation of x-ray radiation from the XeKrArI jet in the spectral region 1.4 – 9 keV confirmed our previous result that such a jet emitted x-rays anisotropically with maximum radiated energy perpendicular to laser beam polarization (typical result demonstrated in Fig. 10). The anisotropy of x-ray emission intensity from XeKrArI varied in different spectral regions: it is smaller for softer x-rays (> 1.4 keV, > 2.4 keV) and rising with increasing photon energy (> 3.5 keV and > 9 keV).

The peak of the electron beam current measured with a Faraday cup (electron cut-off energy >19 keV) was about 0.6 kA. The intensity of the electron beam was anisotropic too: it was stronger along z-axis than near horizontal 15° direction. These data were compared with results of measurements with the 15%Kr/85%Ar jet. The latter has shown a lower peak of the electron beam

current of 0.2 kA. The intensity of the 15%Kr/85%Ar jet electron beam was anisotropic also: stronger in near horizontal 15° direction than in vertical direction. Note, that the peaks of the electron beams were correlated in time with the x-ray bursts for both jet types.

We also investigated the impact of the laser pulse contrast on the gas cluster/jet plasmas. We studied x-ray emission from XeKrArI jet with two values of laser pulse contrast: 10^5 and 10^7. The results were unexpected because typically a higher x-ray yield corresponds to the higher contrast level [1, 10, 11]. It was found that the x-ray yield depends insignificantly on the laser pulse contrast in experiments with the XeKrArI jet (examples of results are demonstrated in Fig. 11, time delay 1000 μs and in Fig.12, time delay 830 μs). For time delay 1000 μs, yields for contrast $K=10^5$ were several percent higher than for $K=10^7$ in the softer spectral region (>1.4 keV), and close or lower in the harder x-ray region (>3.5 keV), except near 9 keV where it was 40 % lower. On the other hand, the comparison of yields from XeKrArI jets with shorter time delay (830 μs) for shot #1600 ($K=10^5$)

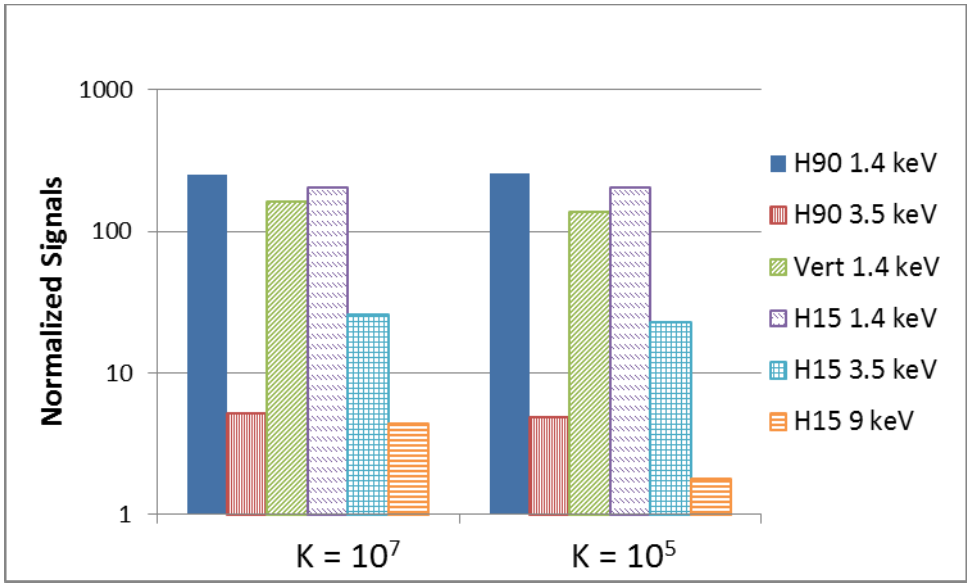

Fig. 11. (Color on-line). Example of normalized spectral integrated distribution of x-ray emission from XeKrArI jets in wide spectral range at 350 fs laser beam intensity 10^{19} W/cm^2 with different laser pulse contrast $K=10^7$ (shot #1583) and $K=10^5$ (shot #1601). Vertical axis shows x-ray intensity in arbitrary units, horizontal axis shows x-ray photons energy in keV. At the right are signs of x-ray detectors groups. Delay time 1000 μs, backing pressure 600 psi.

and shot #1588 ($K=10^7$) has shown that yields for laser pulse contrast $K=10^5$ were several percent lower or similar to those for $K=10^7$ in the softer spectral region (>1.4 keV, > 2.4 keV) and were similar or a little higher in the harder x-ray region (> 3.5keV). In the hard x-ray region above 9 keV, the yield was much higher for contrast $K=10^5$ than for contrast $K=10^7$. This result pointed to the fact that by changing the time delay we can find a regime when harder x-ray emission (> 9 keV) from XeKrAr jets is more intense for lower laser pulse contrast $K=10^5$ than for higher contrast $K=10^7$.

That may offer a practical way to tune the type of radiation that is emitted by changing the time delay and therefore the initial density at the focus spot which can be considered an advantage unique to gas jet targets. Note, that similar results were obtained in experiments with 15% Kr / 85% Ar mixture jets.

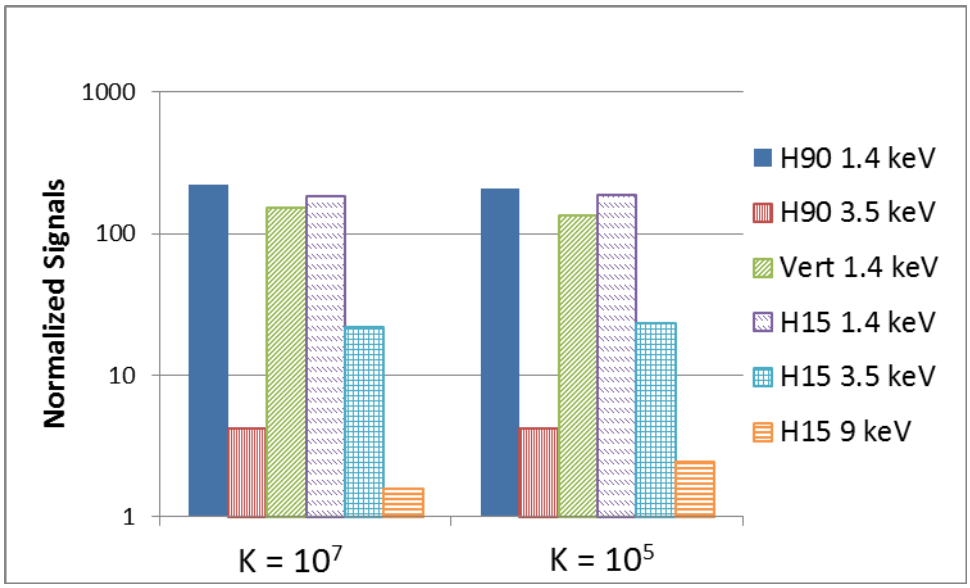

Fig. 12. (Color on-line). Example of normalized spectral integrated distribution of x-ray emission from XeKrArI jet in wide spectral range at 350 fs laser beam intensity 10^{19} W/cm^2 with different laser pulse contrast K=10^7 (shot #1588) and K= 10^5 (shot #1600). Vertical axis shows x-ray intensity in arbitrary units, horizontal axis shows x-ray photon energy in keV. At the right are types of x-ray detector groups. Delay time 830 μs, backing pressure 600 psi.

VI. Discussion and conclusion.

X-ray emission from a debris-free gas-puff x-ray source using Xe, Kr/Ar and Xe/Kr/Ar jets irradiated by sub-ps laser pulses at a laser intensity of 10^{19} W/cm^2 was studied. One of the most intriguing results was that the largest x-ray yield was observed from the Xe/Kr/Ar mixture jet with relatively low Xe and Kr concentrations which was higher than that from both Kr/Ar mixture and pure Xe. The initial idea about increasing the x-ray generation efficiency of the Xe/Kr/Ar mixture was based on the premise that cluster formation at the laser focus spot may be enhanced by adding an impurity gas (Kr and Xe) with lower ionization potential of outer electronic shell compared to the main carrier gas (Ar). We surmised that the interaction of laser with clusters in the jet can lead to higher energy absorption, higher charge states and density of electrons and thus the increase of x-ray emission. Indeed, we obtained experimental confirmation that the utilization of a mixture of gases instead of single gas is more effective and leads to higher x-ray yield. It appears to contradict the Rayleigh scattering data (chapter III) that shows a significantly larger scattering signal from pure Xe

gas. This fact needs additional interpretation in future work. Previously, it was determined that Ar does not cluster in mixtures with Kr [9]; it is also postulated that in the Xe/Kr/Ar mixtures, Xe and Kr cluster independently of each other. The estimation of the maximum conversion coefficient of laser energy to x-rays in the 1.4-3.5 keV spectral region indicated that for the Xe/Kr/Ar mixture it is on the order of $\varepsilon > 3 \times 10^{-4}$. If considered over a wider spectral region, >0.7 keV, the conversion efficiency for the same jet is $\varepsilon \sim 10^{-3}$ that was found in preliminary experiments with Xe/Kr/Ar mixture jet.

Supporting our initial expectations, we experimentally found that xenon plays a significant role in the generation of the strongest x-ray bursts from studied jets (particularly from Xe/Kr/Ar mixtures) and a broader radiated x-ray spectral range compared to pure gas jets, despite Xe relatively low concentration in the mixtures. Numerical simulations with the Molecular Dynamics (MD) code indicate that the xenon clusters survive only a period much shorter than the laser pulse. Laser heating and Coulomb explosion disassemble the clusters in the laser focal spot on a time scale of 100 fs, compared with the 350 fs laser pulse duration. Despite the clusters short life time, that ultimately results in a low-density plasma, they can absorb a large fraction of the laser radiation. Optical field ionization and collisional ionization generate highly charged ions (with ion charge up to q=46) and the hot dense plasma inside the cluster that augments the x-ray emission. For t >100-120 fs the x-ray generation is the result of a laser pulse interaction with hot, low density Xe plasma.

X-ray yields from high and low contrast laser pulses were compared in order to elucidate the impact of the laser pulse pedestal. Contrary to expectations, it was found that x-ray yields for laser pulse with a contrast of $K=10^5$ were close to yields for $K=10^7$ in wide spectral region 1.4-9 keV for both Xe/Kr/Ar and Kr/Ar mixtures jets. A possible explanation of this effect is that, specifically for Xe/Kr/Ar and Kr/Ar mixtures, energy of the laser pulse pedestal ($K=10^5$) was not sufficient to significantly reduce the clusters concentration. In this case, the total x-rays emitted by Xe and Kr clusters and hot low density plasma was not changed significantly compared with higher contrast $K=10^7$.

Another intriguing result was that the x-ray radiation from Xe/Kr/Ar jet is emitted anisotropically, with maximum emission radiated perpendicular to the laser beam polarization. The temperature of the plasma bulk (that connected with slope of x-ray integrated intensity distribution to photon energy axis) was also anisotropic; it was higher in direction orthogonal to the laser beam polarization. The observed anisotropy could be explained by excitation of plasma's electrons oscillations in the direction of the laser electric field polarization. This would give rise to dipole

radiation that is strongest orthogonal to the laser beam polarization direction [18, 19] as we observed in experiments. Another possible explanation can be connected with initial asymmetry of ionized gas distribution in a linear jet and absorption and reemission of x-rays from laser plasma generated inside jet [19].

In summary, it was found that highly non-uniform plasma generated during the interaction of sub-ps laser pulses with Xe/Kr/Ar mixture linear jet is a strong source of x-rays. Non-LTE models have been implemented to analyze the spectroscopic data aided by 3D molecular dynamic simulations of Xe clusters irradiated by sub-ps laser pulses. The observed shape of the x-ray pulses from linear jets, with a sharp forefront and gently sloping trailing edge, was explained with molecular dynamic code. Evidence of electron beam generation in linear jet plasma was found. We established experimentally that the gas-puff x-ray source is indeed debris-free, which is critical for many applications. At laser intensity near 10^{19} W/cm^2 it can generate x-ray pulses in a high repetition regime (up to 10 – 100 Hz) with conversion efficiency of laser energy into X-rays ~ 0.03 - 0.1 % (at 10^{19} W/cm^2). This is clearly a great advantage as opposed to sources using solid laser targets.

Acknowledgements

This work was supported by the Defense Threat Reduction Agency, Basic Research Award #HDTRA1-13-1-0033, to University of Nevada, Reno, and in part by NNSA under DOE Cooperative Agreements DE-NA0001984 and DE-NA0002075. Work by G.M. Petrov was supported by the Naval Research Laboratory 6.1 Base Program.

References.

[1] K.Y. Kim, H.M. Milchberg, A.Ya. Faenov, A.I. Magunov, T.A. Pikuz, I.Yu. Skobelev, Phys. Rev. E **73**, 066403 (2006).

[2] T. Ditmire, T. Donnelly, A.M. Rubenchik, R.W. Falcone, M.D. Perry, Phys. Rev. A **53**, 3379 (1996).

[3] S. Bagchi, P.P. Kiran, K. Yang, A.M. Rao, M.K. Bhuyan, M. Krishnamurthy, G.R. Kumar, Phys. Plasmas **18**, 014502 (2011).

[4] A.Ya. Faenov, I.Yu. Skobelev, T.A. Pikuz, V.E. Fortov, A.S. Boldarev, V.A. Gasilov, L.M. Chen, L. Zhang, W.C. Yan, D.W. Yuan *et. al.,* JETP Lett. **94**, 171 (2011).

[5] P. Koester, G.C. Bussolino, G. Cristoforetti, A. Faenov, A. Giulietti, D. Giulietti, L. Labate, T. Levato, T. Pikuz, L.. Gizzi, Laser and Particle Beams **33**, 331 (2015).

[6] N.L. Kugland, P. Neunayer, T. Doppner, H.-K. Chung, C.G. Constantin, F. Girard, S.H. Glenzer, A. Kemp, C. Niemann, Rev. Sci. Istrum. **79**, 10E917 (2008).

[7] T. Ditmire, P.K. Patel, R.A. Smith, J.S. Wank, S.J. Rose, D. Milathianaki, R.S. Marjoribanks, M.H.R. Hutchison, J. Phys. B., **31**, 2825 (1998).

[8] H. Honda, E. Mura, K. Katsura, E. Takahashi, K. Kondo, Phys. Rev. A. **61,** 023201 (2000).

[9] V.L. Kantsyrev, K.A. Schultz , V.V. Shlyaptseva, A.S. Safronova, I.K. Shrestha, G.M. Petrov, J.J. Moschella, E.E. Petkov, A. Stafford, M.C. Cooper *et al.,* High Energy Density Phys. **19**, 11 (2016).

[10] F. Dorchies, T. Caillaud, F. Blanco, C. Bonte, H. Jouin, S. Micheau, B. Pons, J. Stevefelt*,* Phys. Rev. E, **71**, 066410 (2005).

[11] Th. Fennel, K.H. Meiwes-Broer, J. Tiggesbaumker, P.-G. Reinhard, P.M. Dinh, E. Suraud, Rev. Mod. Phys. **82**, 1793 (2010).

[12] O. Abraham, S.-S. Kim, G.D. Stein, J. Chem. Phys. **75**, 402 (1981).

[13] I. Last, I. Schek, J. Jortner, J. Chem. Phys. **107**, 6685 (1997).

[14] K.Y. Kim, V. Kumarappan, H.M. Milchberg, Appl. Phys. Lett. **83**, 3210 (2003).

[15] A.S. Safronova, V.L. Kantsyrev, A.Y. Faenov, U.I. Safronova, P. Wiewior, N. Renard-LeGalloude, A. A. Esaulov, M.E. Weller, A. Stafford, P. Wilcox *et al*., High Energy Density Phys. **8,** 190 (2012).

[16] G.M. Petrov, J. Davis, A.L. Velikovich, P.C. Kepple, A. Dasgupta, R.W. Clark, A.B. Borisov, K. Boyer, C.K. Rhodes, Phys. Rev. E **71**, 036411 (2005).

[17] G. M. Petrov, J. Davis, A.L. Velikovich, P.C. Kepple, A. Dasgupta, R.W. Clark, Phys. Plasmas **12**, 063103 (2005).

[18] O.N. Krokhin, Yu.A. Mikhailov, V.V. Pustovalov, A.A. Rupasov, V.P. Silin, G.V. Sklizkov, A.S. Shikanov, JETP Lett. **20**, 105 (1974).

[19] S. Kranzusch, C. Peth, K. Mann, Rev. Sci. Istrum.**74**, 969 (2003).